

1 Simulation setup

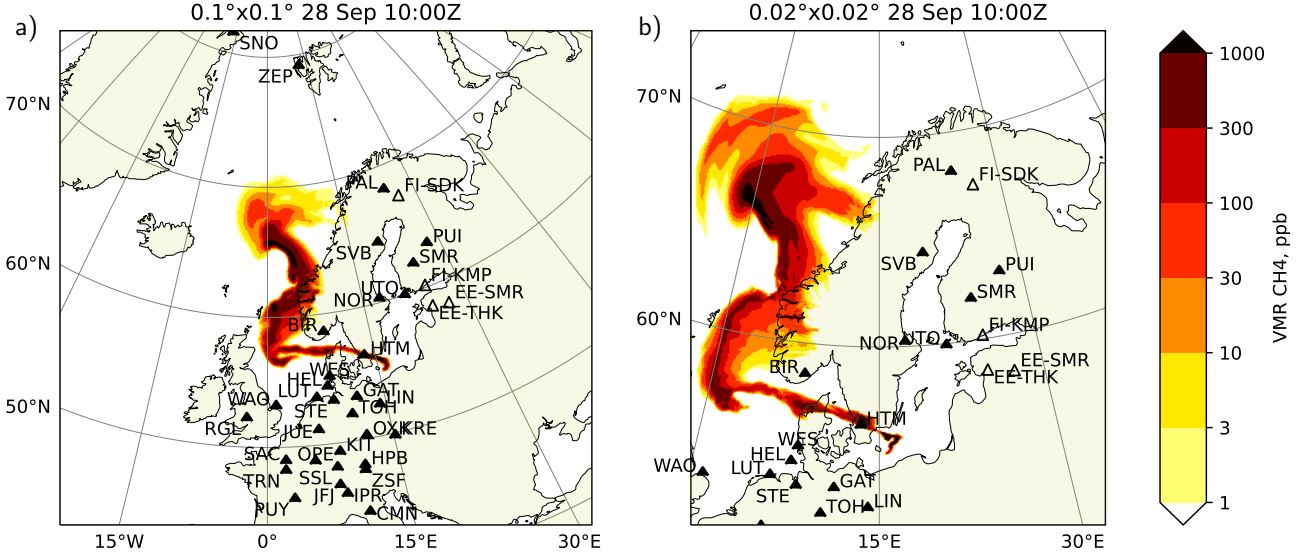


Figure S1. Simulation domains used for the study, and locations of the observation stations. ICOS stations shown with filled symbols.

The simulations were performed with Silam model on two domains shown in Fig. S1. The larger domain was simulated at 0.1-deg and 0.4-deg resolution (Fig. S1a) driven with the same set of operational ECMWF forecasts, The smaller domain was simulated at 0.02-deg resolution (Fig. S1b), with MEPS unperturbed-member forecasts with 2.5-km resolution.

5 2 Timeseries for Stations

This section shows simulated and observed timeseries for the stations that did not fit to the main paper and Taylor diagrams for them.

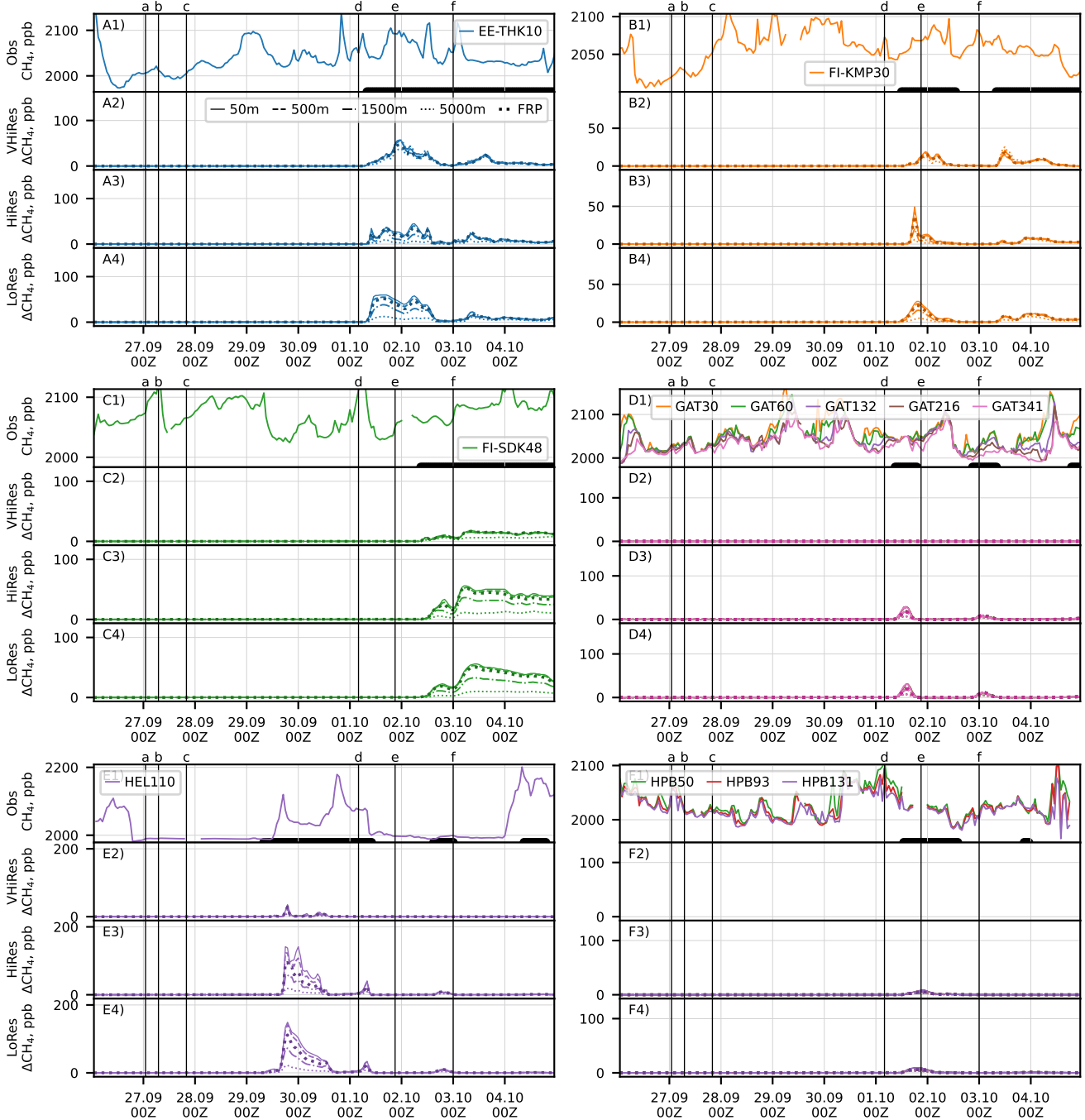


Figure S2. Timeseries of methane mixing ratio observed at EE-THK, FI-KMP, FI-SDK, GAT, HEL and HPB stations after the pipeline rupture, and corresponding timeseries simulated with three different resolutions for several vertical profiles of the release. Each group of panels corresponds to a station. The panels in each group are (top down) for observations, and model with 0.02-deg, 0.1-deg, 0.4-deg resolution. Measurement heights are coded with colors, and emission heights with line styles. Vertical lines mark the moments shown in maps of the main paper

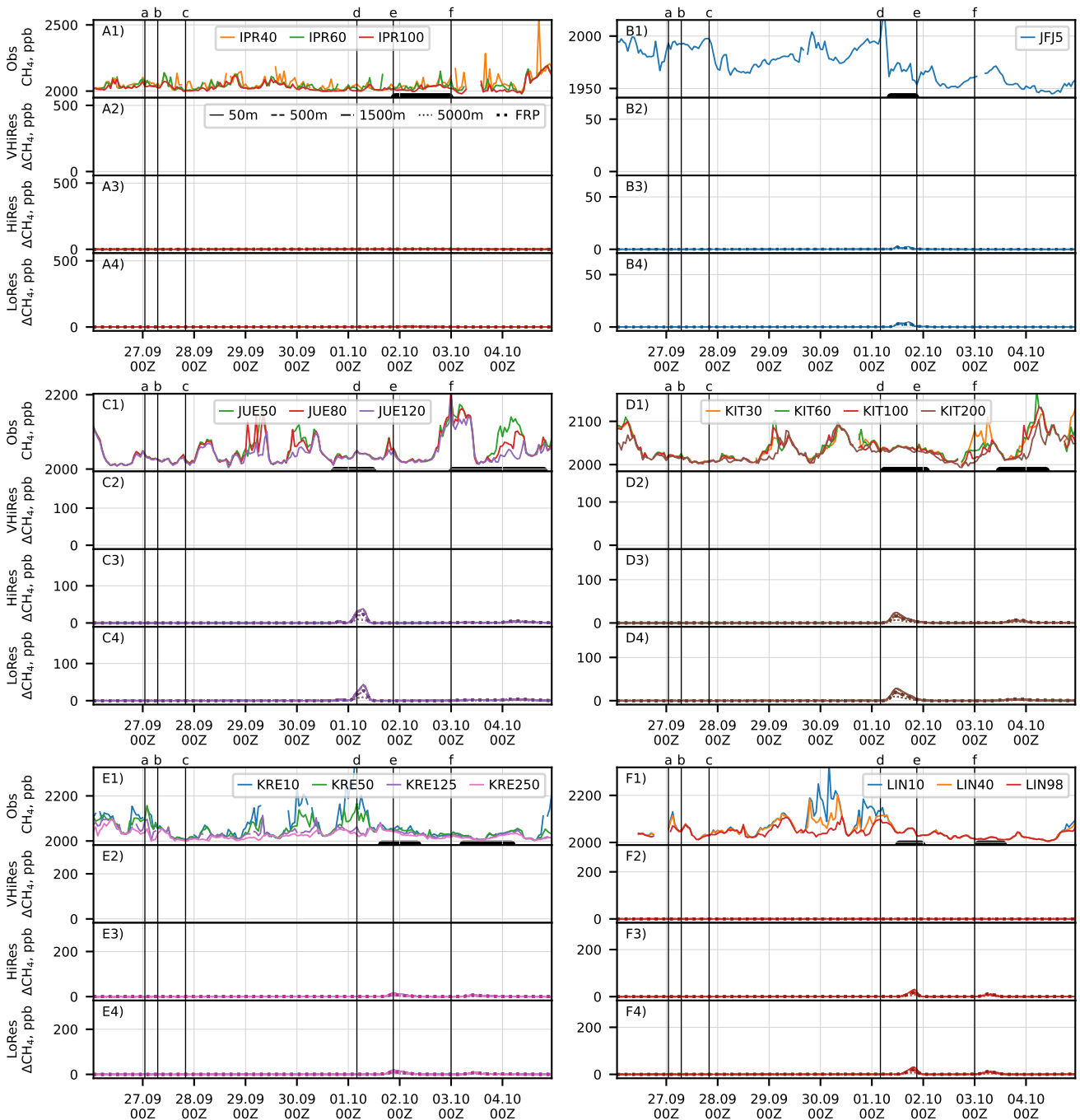


Figure S3. Timeseries of methane mixing ratio observed at IPR, JFJ, JUE, KIT, KRE, and LIN stations after the pipeline rupture, and corresponding timeseries simulated with three different resolutions for several vertical profiles of the release. Each group of panels corresponds to a station. The panels in each group are (top down) for observations, and model with 0.02-deg, 0.1-deg, 0.4-deg resolution. Measurement heights are coded with colors, and emission heights with line styles. Vertical lines mark the moments shown in maps of the main paper

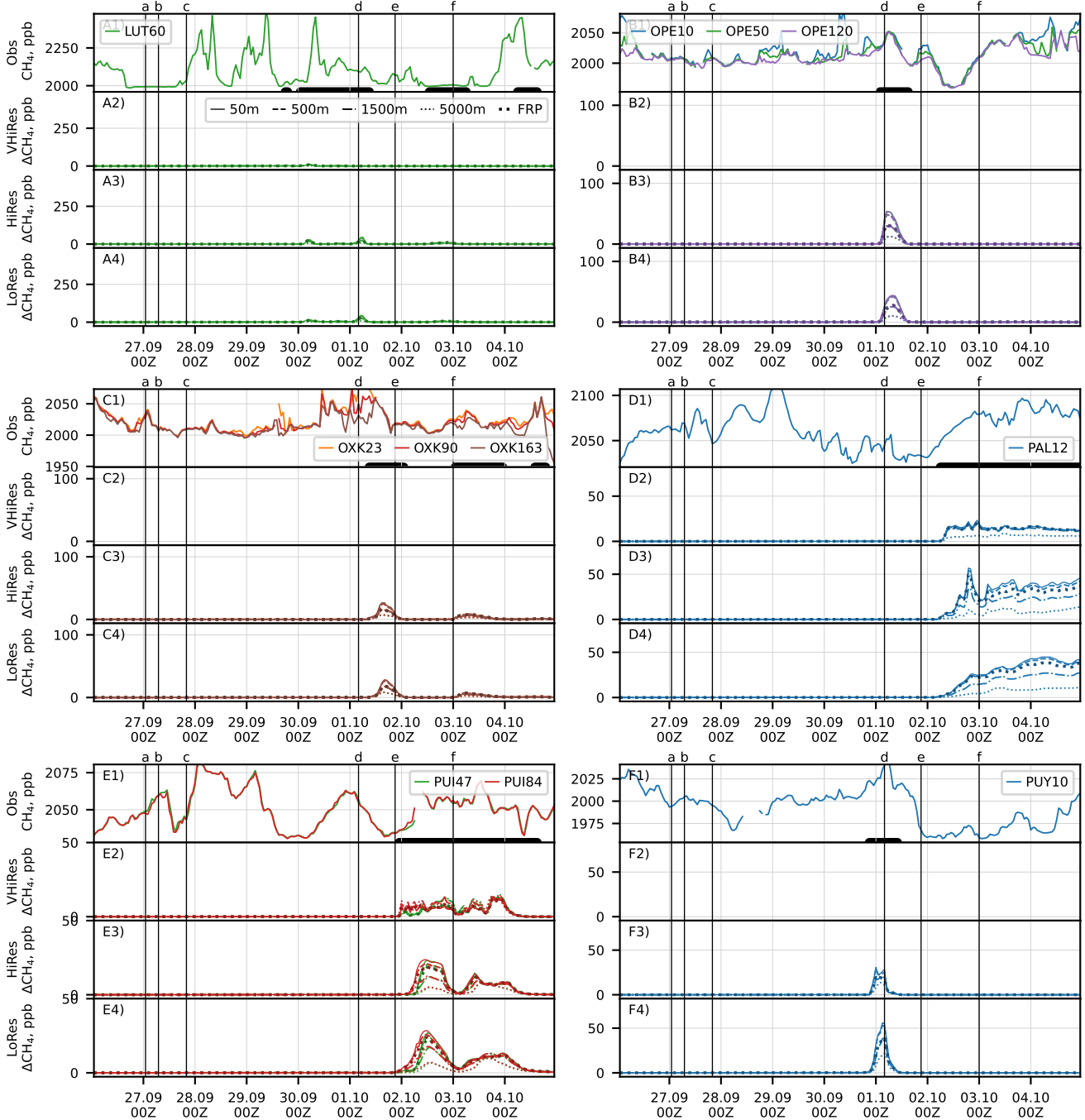


Figure S4. Timeseries of methane mixing ratio observed at LUT, OPE, OXK, PAL, PUI, and PUY stations after the pipeline rupture, and corresponding timeseries simulated with three different resolutions for several vertical profiles of the release. Each group of panels corresponds to a station. The panels in each group are (top down) for observations, and model with 0.02-deg, 0.1-deg, 0.4-deg resolution. Measurement heights are coded with colors, and emission heights with line styles. Vertical lines mark the moments shown in maps of the main paper

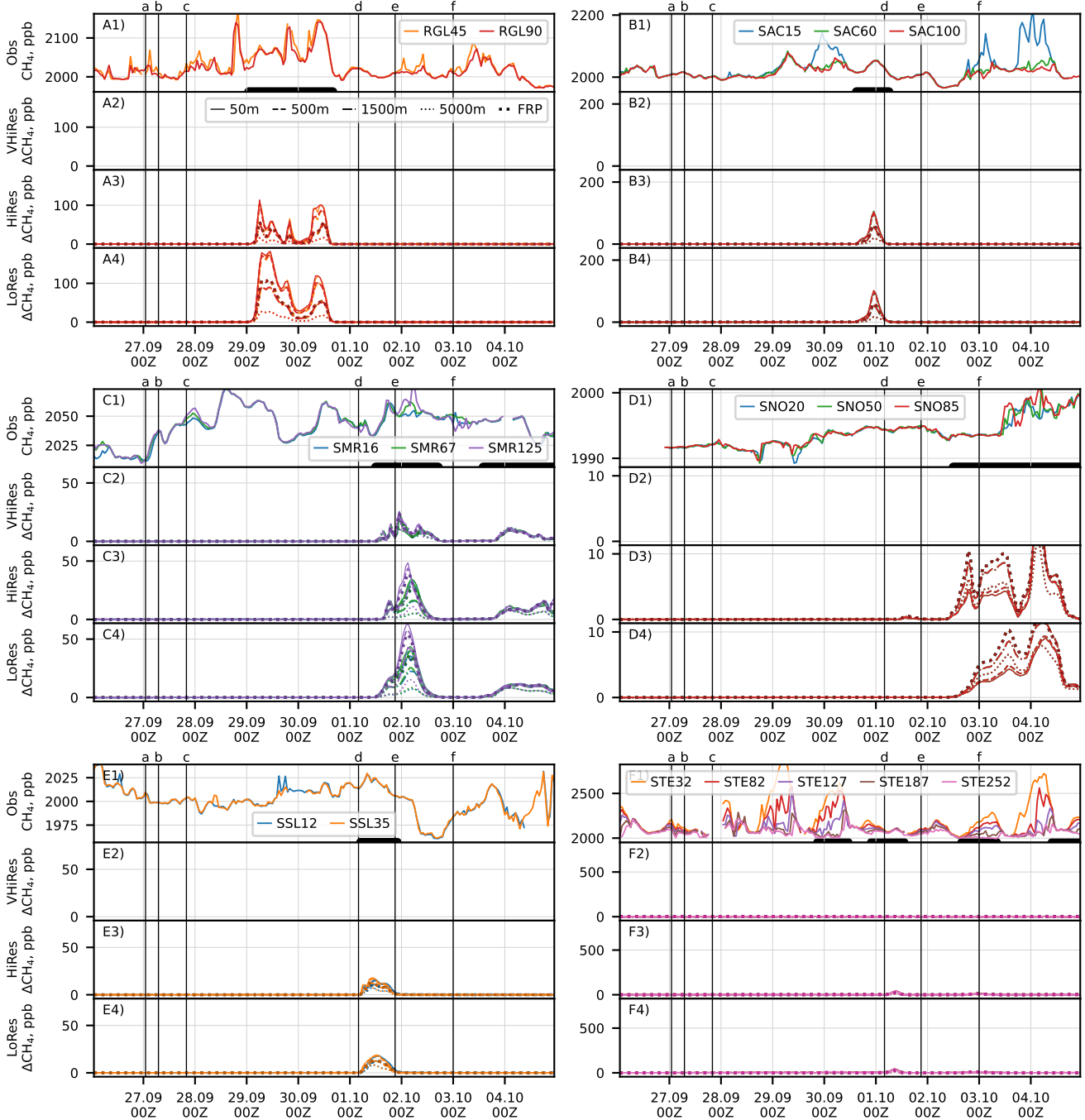


Figure S5. Timeseries of methane mixing ratio observed at RGL, SAC, SMR, SNO, SSL, and STE stations after the pipeline rupture, and corresponding timeseries simulated with three different resolutions for several vertical profiles of the release. Each group of panels corresponds to a station. The panels in each group are (top down) for observations, and model with 0.02-deg, 0.1-deg, 0.4-deg resolution. Measurement heights are coded with colors, and emission heights with line styles. Vertical lines mark the moments shown in maps of the main paper

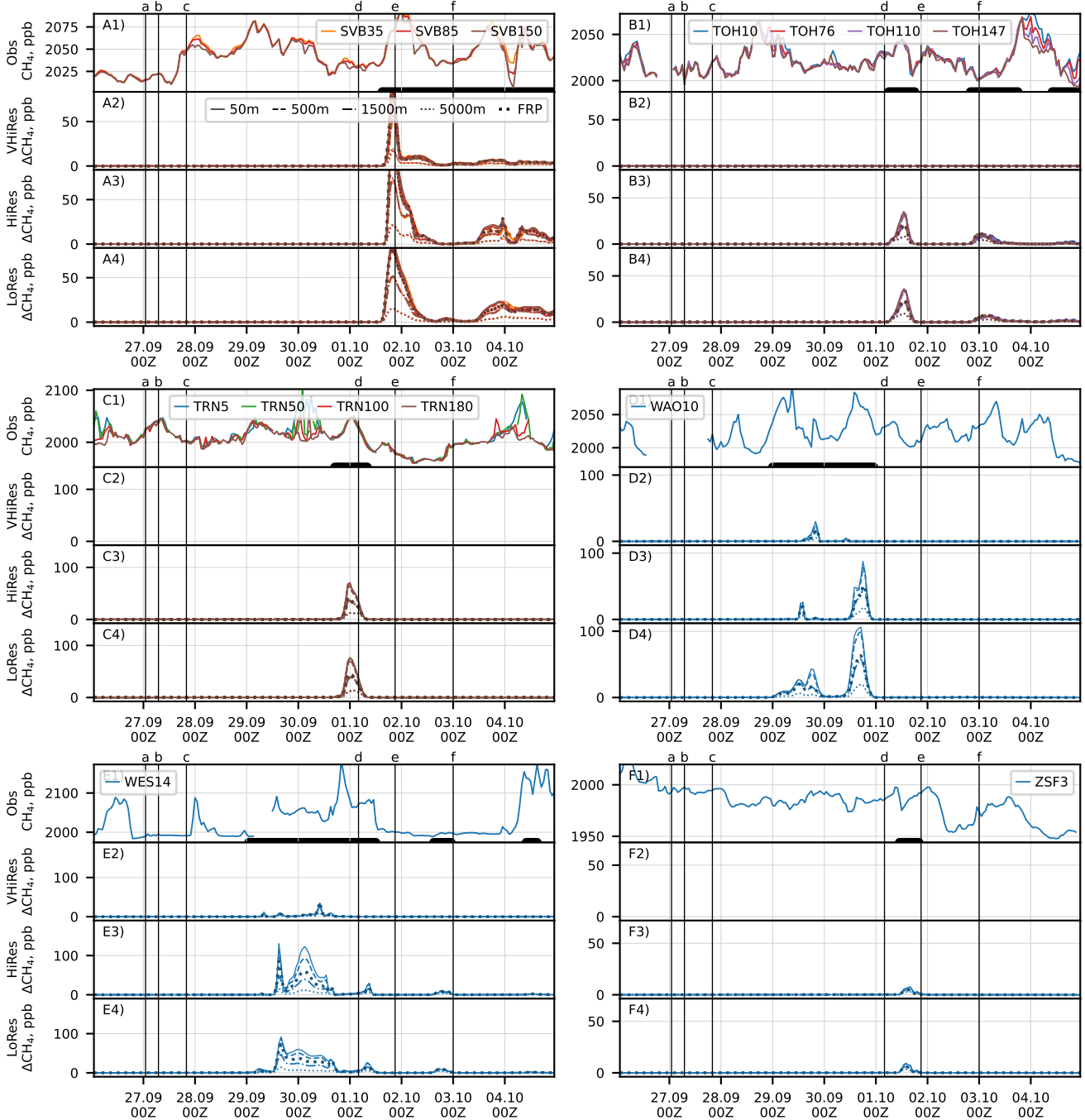


Figure S6. Timeseries of methane mixing ratio observed at SVB, TOH, TRN, WAO, WES, and ZSF stations after the pipeline rupture, and corresponding timeseries simulated with three different resolutions for several vertical profiles of the release. Each group of panels corresponds to a station. The panels in each group are (top down) for observations, and model with 0.02-deg, 0.1-deg, 0.4-deg resolution. Measurement heights are coded with colors, and emission heights with line styles. Vertical lines mark the moments shown in maps of the main paper

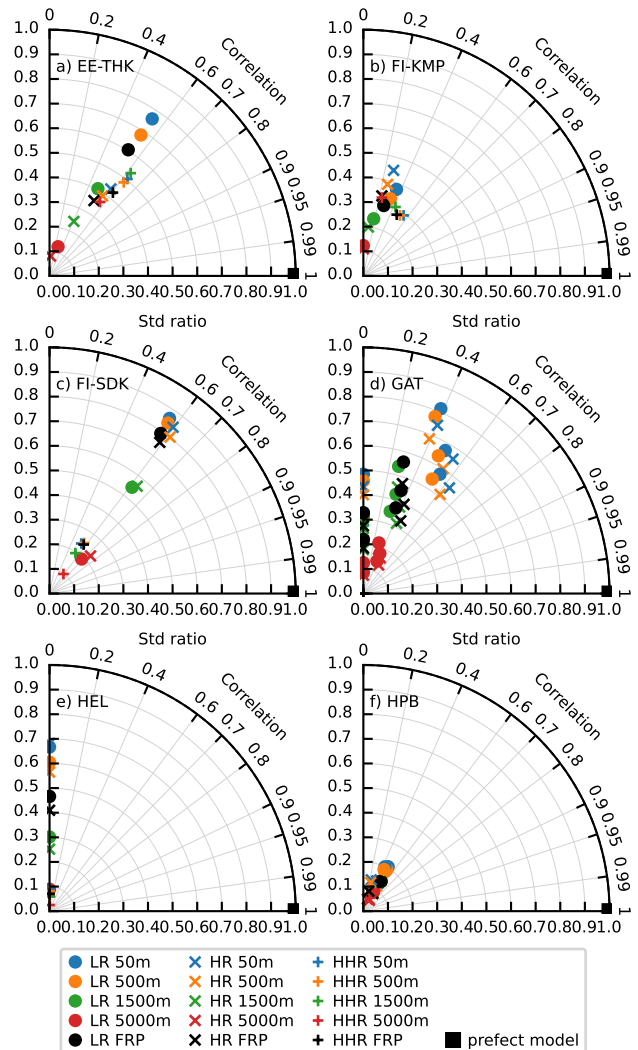


Figure S7. Taylor diagrams of model performance on the timeseries shown in Fig. S2

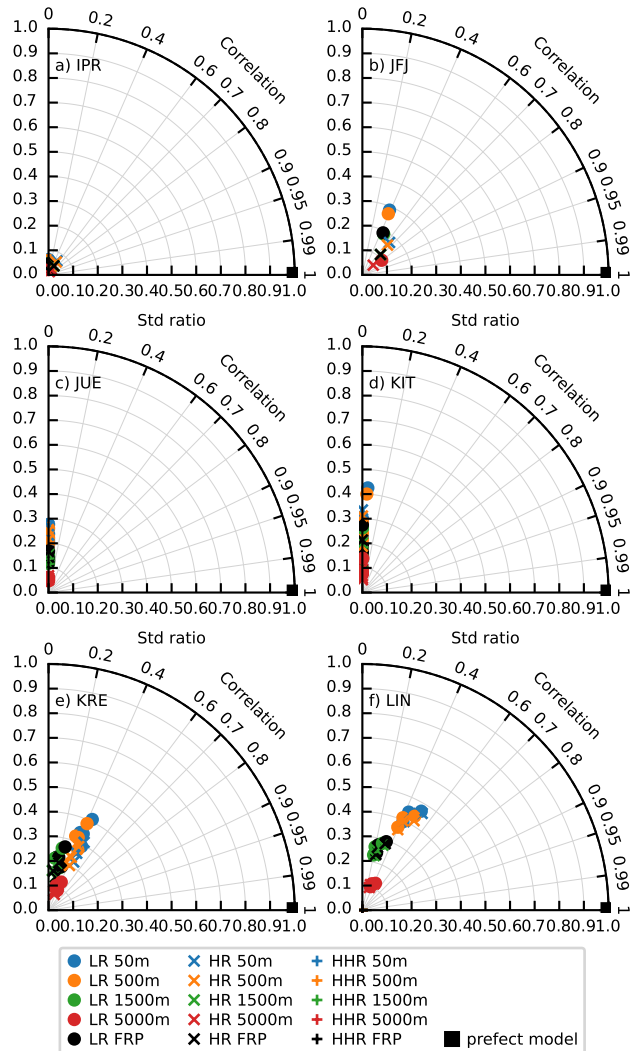


Figure S8. Taylor diagrams of model performance on the timeseries shown in Fig. S3

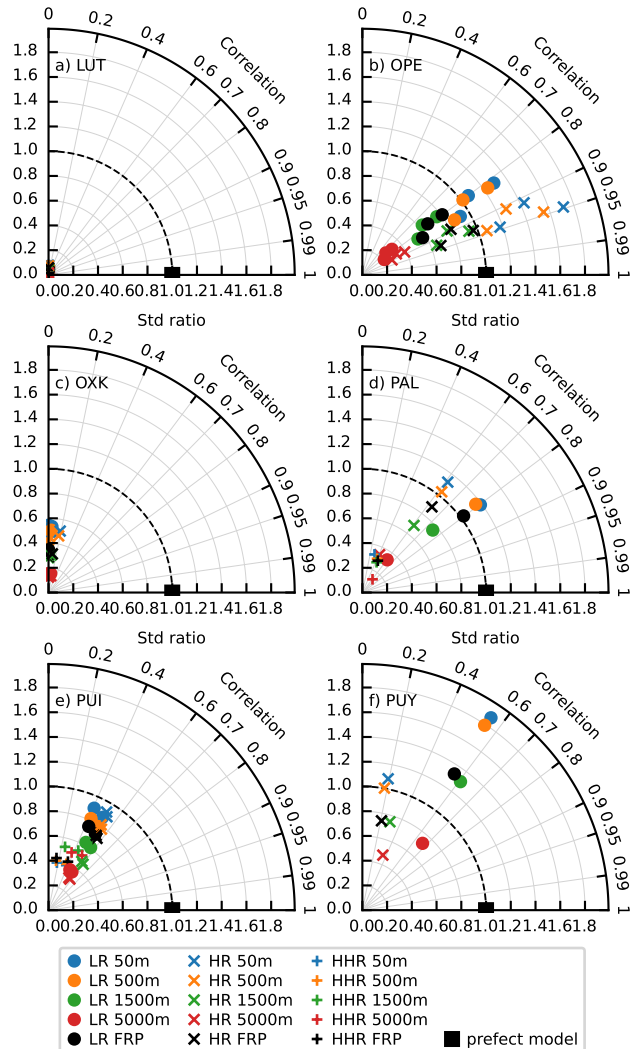


Figure S9. Taylor diagrams of model performance on the timeseries shown in Fig. S4

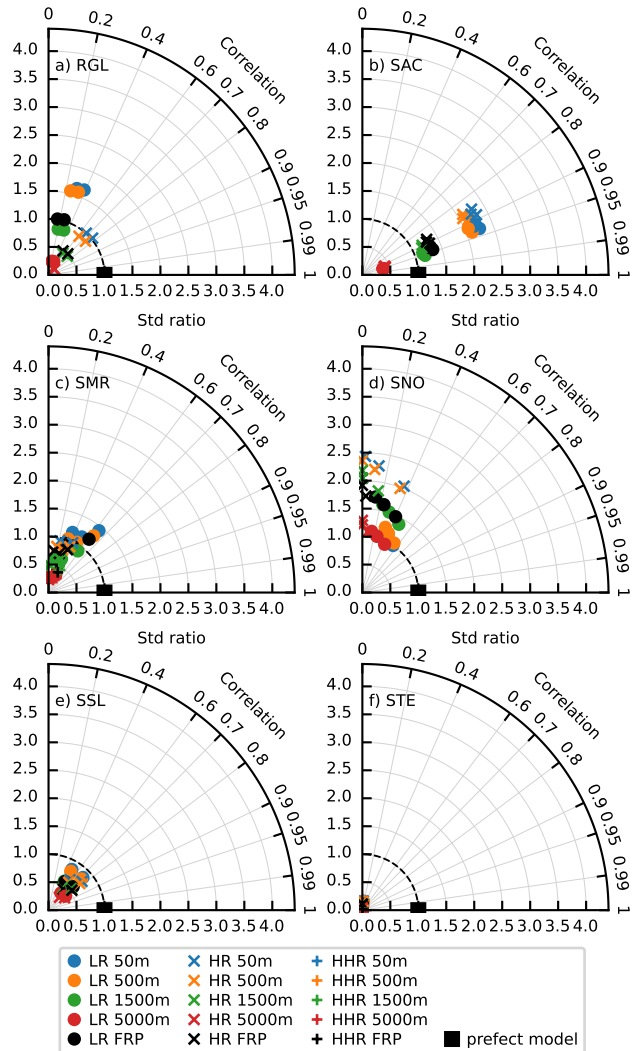


Figure S10. Taylor diagrams of model performance on the timeseries shown in Fig. S5

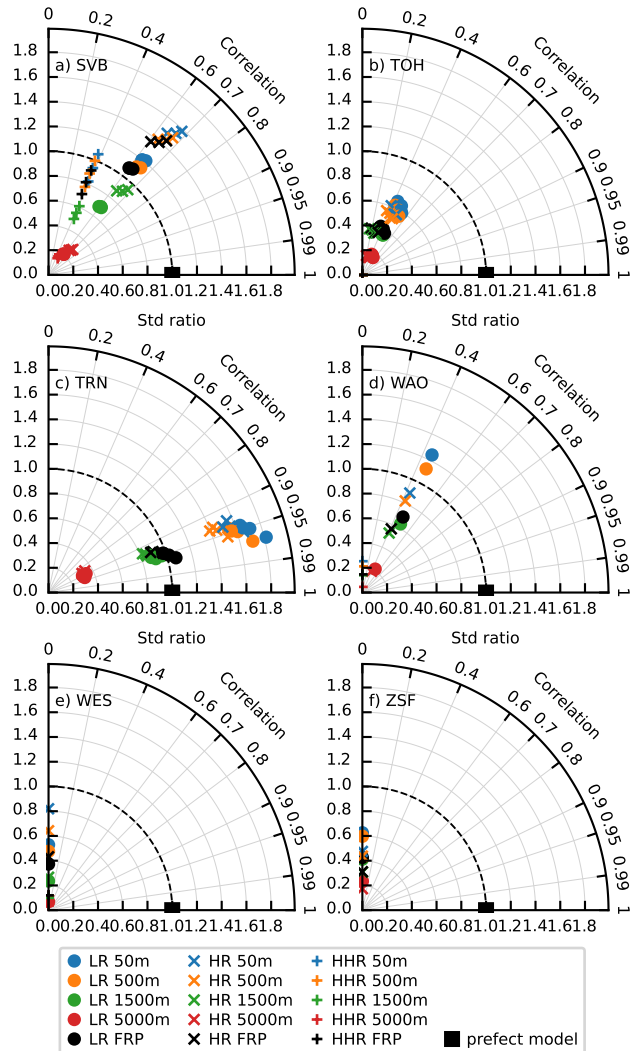


Figure S11. Taylor diagrams of model performance on the timeseries shown in Fig. S6

3 LES sensitivity simulations

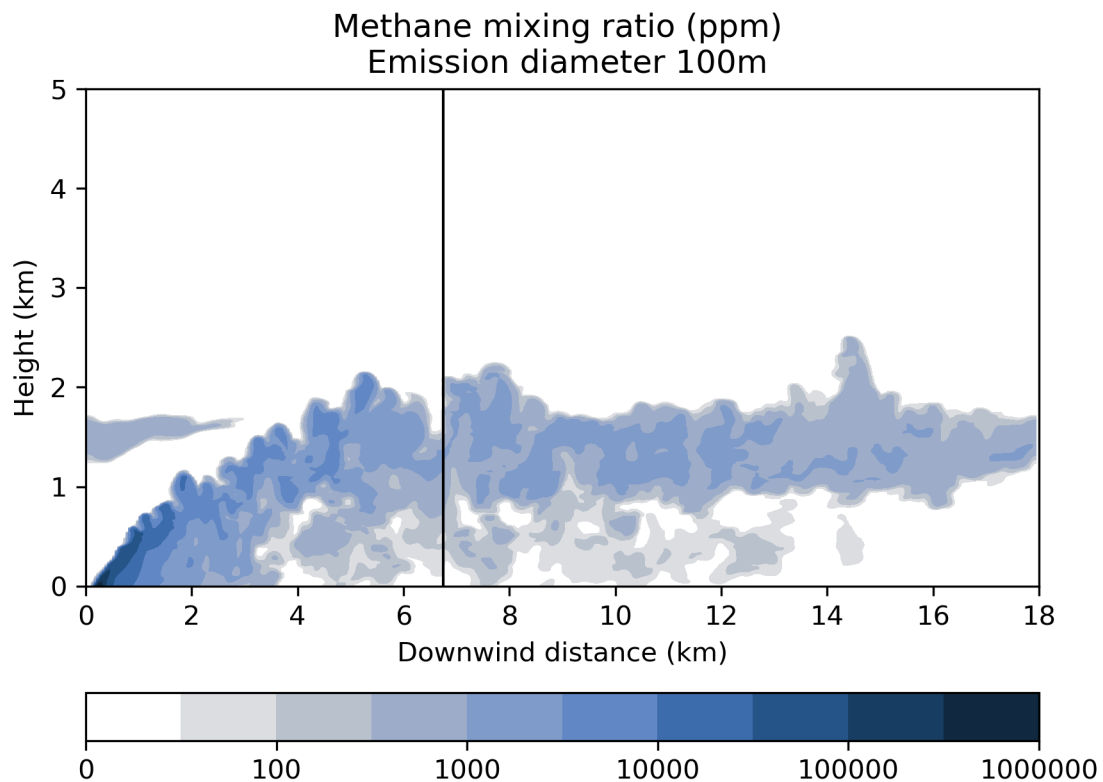


Figure S12. Methane mixing ratio in the central line of the LES simulated plume for the maximum methane release from a circle with 100 m diameter. The vertical line indicates the point where the plume rise has finished.

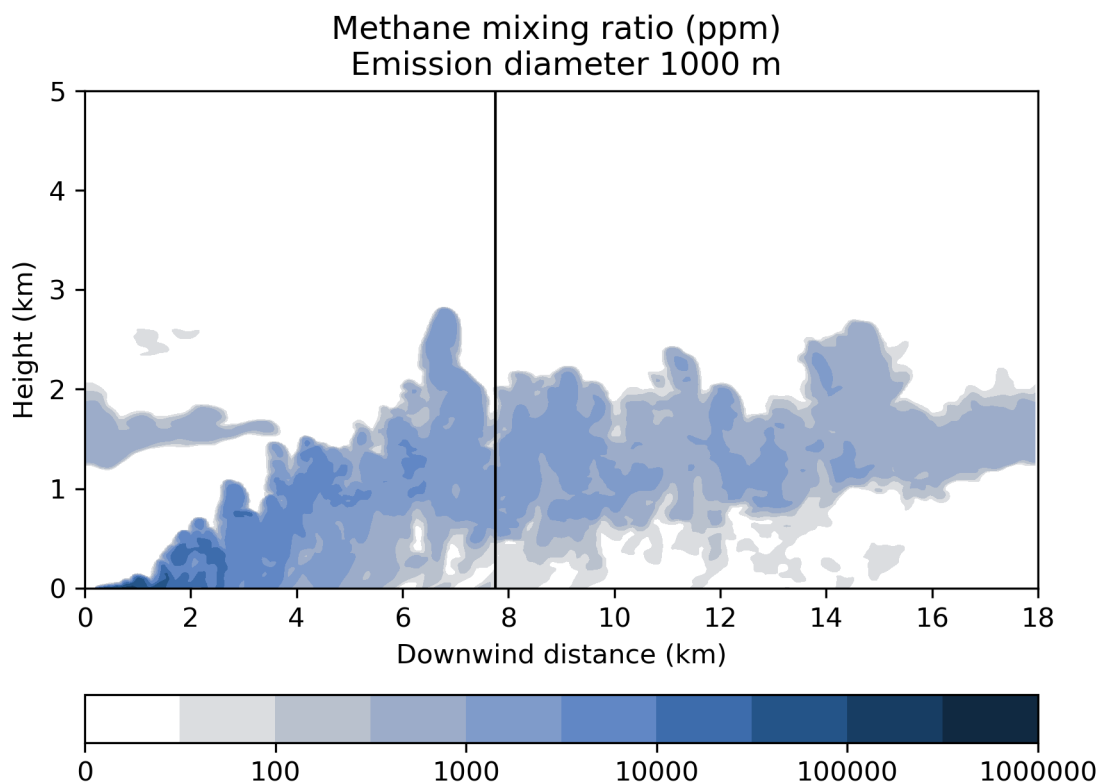


Figure S13. LES simulated plume for the maximum methane release from a circle with 1000 m diameter.

4 Acknowledgments for ICOS data

- 10 The ICOS data usage policy (<https://www.icos-cp.eu/data-services/about-data-portal/data-license>, accessed 30.11.2022) requires each publication to have a reference for each of the time series used for a study, and the references are different for each measurement height at each station. The table below is intended to fulfill this requirement:

Code	References
BIR	Lund Myhre, C., Platt, S. M., Lunder, C., and Hermansen, O.: ICOS ATC NRT CH4 growing time series, Birkenes (10.0m), 2022-03-01–2022-10-16, https://hdl.handle.net/11676/a-OqGFe7Aga6-k7CHen39EyQ , 2022
	Lund Myhre, C., Platt, S. M., Lunder, C., and Hermansen, O.: ICOS ATC NRT CH4 growing time series, Birkenes (50.0m), 2022-03-01–2022-10-16, https://hdl.handle.net/11676/QhtU7Bpi3hW63r_P_YRETTsU , 2022
GAT	Lund Myhre, C., Platt, S. M., Lunder, C., and Hermansen, O.: ICOS ATC NRT CH4 growing time series, Birkenes (75.0m), 2022-03-01–2022-10-16, https://hdl.handle.net/11676/M1WVYeDMy6UtPnSvF6KKmq_L , 2022
	Kubistin, D., Plaß-Dülmer, C., Kneuer, T., Lindauer, M., and Müller-Williams, J.: ICOS ATC NRT CH4 growing time series, Gartow (30.0m), 2022-03-01–2022-10-16, https://hdl.handle.net/11676/V9y--C-FvYXizfojwVq3bw42 , 2022
HEL	Kubistin, D., Plaß-Dülmer, C., Kneuer, T., Lindauer, M., and Müller-Williams, J.: ICOS ATC NRT CH4 growing time series, Gartow (60.0m), 2022-03-01–2022-10-16, https://hdl.handle.net/11676/Yk1xCKJYJSz_GWeATpDA3Rjt , 2022
	Kubistin, D., Plaß-Dülmer, C., Kneuer, T., Lindauer, M., and Müller-Williams, J.: ICOS ATC NRT CH4 growing time series, Gartow (132.0m), 2022-03-01–2022-10-16, https://hdl.handle.net/11676/Rt04d54lFTra9RYcYIGPQN5H , 2022
HPB	Kubistin, D., Plaß-Dülmer, C., Kneuer, T., Lindauer, M., and Müller-Williams, J.: ICOS ATC NRT CH4 growing time series, Gartow (216.0m), 2022-03-01–2022-10-16, https://hdl.handle.net/11676/_qPTkWsLArD9RYD1s8gorAM0 , 2022
	Kubistin, D., Plaß-Dülmer, C., Kneuer, T., Lindauer, M., and Müller-Williams, J.: ICOS ATC NRT CH4 growing time series, Gartow (341.0m), 2022-03-01–2022-10-16, https://hdl.handle.net/11676/K5H4gA-BlsJEyT2g8NsCnW9x , 2022
HTM	Kubistin, D., Plaß-Dülmer, C., Kneuer, T., Lindauer, M., and Müller-Williams, J.: ICOS ATC NRT CH4 growing time series, Helgoland (110.0m), 2022-03-01–2022-10-16, https://hdl.handle.net/11676/_NblFnzvy2GGTPpdD0_SpKn- , 2022
	Kubistin, D., Plaß-Dülmer, C., Kneuer, T., Lindauer, M., and Müller-Williams, J.: ICOS ATC NRT CH4 growing time series, Hohenpeissenberg (50.0m), 2022-03-01–2022-10-16, https://hdl.handle.net/11676/tpDePhqI3v9_aql5xksIrf8S , 2022
HTM	Kubistin, D., Plaß-Dülmer, C., Kneuer, T., Lindauer, M., and Müller-Williams, J.: ICOS ATC NRT CH4 growing time series, Hohenpeissenberg (93.0m), 2022-03-01–2022-10-16, https://hdl.handle.net/11676/nXNqErmYi8m2wemDaJz_Z9Dr , 2022
	Kubistin, D., Plaß-Dülmer, C., Kneuer, T., Lindauer, M., and Müller-Williams, J.: ICOS ATC NRT CH4 growing time series, Hohenpeissenberg (131.0m), 2022-03-01–2022-10-16, https://hdl.handle.net/11676/GabqfaCOTkNLQnnjz_lMn_6l , 2022
HTM	Heliasz, M. and Biermann, T.: ICOS ATC NRT CH4 growing time series, Hyltemossa (30.0m), 2022-03-01–2022-10-16, https://hdl.handle.net/11676/l9QSNSWCe3fqCzL0iTwLU8la , 2022
	Heliasz, M. and Biermann, T.: ICOS ATC NRT CH4 growing time series, Hyltemossa (70.0m), 2022-03-01–2022-10-16, https://hdl.handle.net/11676/IV2WF-vf84LsT73z6kWFJgV4 , 2022
	Heliasz, M. and Biermann, T.: ICOS ATC NRT CH4 growing time series, Hyltemossa (150.0m), 2022-03-01–2022-10-16, https://hdl.handle.net/11676/-uYDRenkP8mfYPJLhekmx9Ko , 2022

IPR	Manca, G.: ICOS ATC NRT CH4 growing time series, Ispra (40.0m), 2022-03-01–2022-10-16, https://hdl.handle.net/11676/goYrYu_b3TRzccaCrnviIdJr , 2022
	Manca, G.: ICOS ATC NRT CH4 growing time series, Ispra (60.0m), 2022-03-01–2022-10-16, https://hdl.handle.net/11676/6SNNjI9H053sR6JuOTHvobb , 2022
	Manca, G.: ICOS ATC NRT CH4 growing time series, Ispra (100.0m), 2022-03-01–2022-10-16, https://hdl.handle.net/11676/XaKdSOVJNeCxDzOMPzmUTSck , 2022
JFJ	Emmenegger, L., Leuenberger, M., and Steinbacher, M.: ICOS ATC NRT CH4 growing time series, Jungfraujoch (5.0m), 2022-03-01–2022-10-16, https://hdl.handle.net/11676/k6LNPK_XM3nq3cu_u7wqTo5 , 2022
JUE	Kubistin, D., Plaß-Dülmer, C., Kneuer, T., Lindauer, M., and Müller-Williams, J.: ICOS ATC NRT CH4 growing time series, Jülich (50.0m), 2022-03-01–2022-10-16, https://hdl.handle.net/11676/UkCEbA_UEl0SfhnwslYcsPw , 2022
	Kubistin, D., Plaß-Dülmer, C., Kneuer, T., Lindauer, M., and Müller-Williams, J.: ICOS ATC NRT CH4 growing time series, Jülich (80.0m), 2022-03-01–2022-10-16, https://hdl.handle.net/11676/7bmZAct3TdgB6jcyDMu6PDtp , 2022
	Kubistin, D., Plaß-Dülmer, C., Kneuer, T., Lindauer, M., and Müller-Williams, J.: ICOS ATC NRT CH4 growing time series, Jülich (120.0m), 2022-03-01–2022-10-16, https://hdl.handle.net/11676/LjLTsMHdFxBEBOmM_3VfVo8l , 2022
KIT	Kubistin, D., Plaß-Dülmer, C., Kneuer, T., Lindauer, M., and Müller-Williams, J.: ICOS ATC NRT CH4 growing time series, Karlsruhe (30.0m), 2022-03-01–2022-10-16, https://hdl.handle.net/11676/-LsGIybsjKN9foX5aNZjBgDD , 2022
	Kubistin, D., Plaß-Dülmer, C., Kneuer, T., Lindauer, M., and Müller-Williams, J.: ICOS ATC NRT CH4 growing time series, Karlsruhe (60.0m), 2022-03-01–2022-10-16, https://hdl.handle.net/11676/KdtRIMM7cTWMgiY4gUFdj_xT , 2022
	Kubistin, D., Plaß-Dülmer, C., Kneuer, T., Lindauer, M., and Müller-Williams, J.: ICOS ATC NRT CH4 growing time series, Karlsruhe (100.0m), 2022-03-01–2022-10-16, https://hdl.handle.net/11676/Ptxukrr5xLtFUId8G0HtsIU- , 2022
	Kubistin, D., Plaß-Dülmer, C., Kneuer, T., Lindauer, M., and Müller-Williams, J.: ICOS ATC NRT CH4 growing time series, Karlsruhe (200.0m), 2022-03-01–2022-10-16, https://hdl.handle.net/11676/b9ItM9jOFqwmxoenJdP8qJfE , 2022
KRE	Marek, M., Vítková, G., and Komínková, K.: ICOS ATC NRT CH4 growing time series, Křešín u Pacova (10.0m), 2022-03-01–2022-10-16, https://hdl.handle.net/11676/S9IKaCm185wQ-NnhcVfNr_FV , 2022
	Marek, M., Vítková, G., and Komínková, K.: ICOS ATC NRT CH4 growing time series, Křešín u Pacova (50.0m), 2022-03-01–2022-10-16, https://hdl.handle.net/11676/RH17_H2biGCsAT8YmFLMP_po , 2022
	Marek, M., Vítková, G., and Komínková, K.: ICOS ATC NRT CH4 growing time series, Křešín u Pacova (125.0m), 2022-03-01–2022-10-16, https://hdl.handle.net/11676/03tUv86UaHEN3HfcnMAdRfiC , 2022
	Marek, M., Vítková, G., and Komínková, K.: ICOS ATC NRT CH4 growing time series, Křešín u Pacova (250.0m), 2022-03-01–2022-10-16, https://hdl.handle.net/11676/PCHil9Cvtf_U1WFBOTweAMr , 2022
LIN	Kubistin, D., Plaß-Dülmer, C., Kneuer, T., Lindauer, M., and Müller-Williams, J.: ICOS ATC NRT CH4 growing time series, Lindenberg (10.0m), 2022-03-01–2022-10-16, https://hdl.handle.net/11676/E_1Wtk5M0nPoWUNn2C70x4bA , 2022
	Kubistin, D., Plaß-Dülmer, C., Kneuer, T., Lindauer, M., and Müller-Williams, J.: ICOS ATC NRT CH4 growing time series, Lindenberg (40.0m), 2022-03-01–2022-10-16, https://hdl.handle.net/11676/c-IgTGo-sGfd5M1WkwWsTeO , 2022
	Kubistin, D., Plaß-Dülmer, C., Kneuer, T., Lindauer, M., and Müller-Williams, J.: ICOS ATC NRT CH4 growing time series, Lindenberg (98.0m), 2022-03-01–2022-10-16, https://hdl.handle.net/11676/exzokQZTG4d71_uifabPbE2k , 2022

NOR	Lehner, I. and Mölder, M.: ICOS ATC NRT CH4 growing time series, Norunda (32.0m), 2022-03-01–2022-10-16, https://hdl.handle.net/11676/1hIMjlfGI_pDmu8CLT2DNB4R , 2022 Lehner, I. and Mölder, M.: ICOS ATC NRT CH4 growing time series, Norunda (58.0m), 2022-03-01–2022-10-16, https://hdl.handle.net/11676/vZQwyfmyDbICceVXXeEfe7h , 2022 Lehner, I. and Mölder, M.: ICOS ATC NRT CH4 growing time series, Norunda (100.0m), 2022-03-01–2022-10-16, https://hdl.handle.net/11676/DHD1wLPlqqb2Fo-NIWVBHed5 , 2022
OPE	Ramonet, M., Conil, S., Delmotte, M., Laurent, O., and Lopez, M.: ICOS ATC NRT CH4 growing time series, Observatoire pérenne de l'environnement (10.0m), 2022-03-01–2022-10-13, https://hdl.handle.net/11676/IOygtpKfddma_W3oiuAT1ZwH , 2022 Ramonet, M., Conil, S., Delmotte, M., Laurent, O., and Lopez, M.: ICOS ATC NRT CH4 growing time series, Observatoire pérenne de l'environnement (50.0m), 2022-03-01–2022-10-13, https://hdl.handle.net/11676/z4xqu1w9Z8rnIR0lb4vGHvWF , 2022 Ramonet, M., Conil, S., Delmotte, M., Laurent, O., and Lopez, M.: ICOS ATC NRT CH4 growing time series, Observatoire pérenne de l'environnement (120.0m), 2022-03-01–2022-10-13, https://hdl.handle.net/11676/bZRhd65ajH8SUtOaeQY3Zq8s , 2022
OXK	Kubistin, D., Plaß-Dülmer, C., Kneuer, T., Lindauer, M., and Müller-Williams, J.: ICOS ATC NRT CH4 growing time series, Ochsenkopf (23.0m), 2022-03-01–2022-10-16, https://hdl.handle.net/11676/VGRVLKskMd3dXbp_StcMSV1p , 2022 Kubistin, D., Plaß-Dülmer, C., Kneuer, T., Lindauer, M., and Müller-Williams, J.: ICOS ATC NRT CH4 growing time series, Ochsenkopf (90.0m), 2022-03-01–2022-10-16, https://hdl.handle.net/11676/Z8yAT3JQSwGF1zkhywmq1MG2 , 2022 Kubistin, D., Plaß-Dülmer, C., Kneuer, T., Lindauer, M., and Müller-Williams, J.: ICOS ATC NRT CH4 growing time series, Ochsenkopf (163.0m), 2022-03-01–2022-10-16, https://hdl.handle.net/11676/VGHdiYnPch1Zin7x8VapXcw_ , 2022
PAL	Hatakka, J.: ICOS ATC NRT CH4 growing time series, Pallas (12.0m), 2022-03-01–2022-10-16, https://hdl.handle.net/11676/rdJeKi7QQOsxwQw3VSeNaj-J , 2022
PUI	Lehtinen, K. and Leskinen, A.: ICOS ATC NRT CH4 growing time series, Puijo (47.0m), 2022-03-01–2022-10-16, https://hdl.handle.net/11676/kBDWxEzhukOrauqsMRsEY6EK , 2022 Lehtinen, K. and Leskinen, A.: ICOS ATC NRT CH4 growing time series, Puijo (84.0m), 2022-03-01–2022-10-16, https://hdl.handle.net/11676/DsxourWEp6XbWbHn3NULXXZW , 2022
PUY	Colomb, A., Ramonet, M., Yver-Kwok, C., Delmotte, M., Lopez, M., and Pichon, J.-M.: ICOS ATC NRT CH4 growing time series, Puy de Dôme (10.0m), 2022-03-01–2022-10-16, https://hdl.handle.net/11676/zNBneKJ90Iuba1ByX7RFNQsO , 2022
RGL	O'Doherty, S., Pitt, J., and Stanley, K.: ICOS ATC NRT CH4 growing time series, Ridge Hill (45.0m), 2022-03-01–2022-10-17, https://hdl.handle.net/11676/sD2PTx5XDblG6eeL5XsCJYzC , 2022 O'Doherty, S., Pitt, J., and Stanley, K.: ICOS ATC NRT CH4 growing time series, Ridge Hill (90.0m), 2022-03-01–2022-10-17, https://hdl.handle.net/11676/dtiLBJJH-nU7J5lk_eiD7re9 , 2022
SAC	Ramonet, M., Delmotte, M., and Lopez, M.: ICOS ATC NRT CH4 growing time series, Saclay (15.0m), 2022-03-01–2022-10-16, https://hdl.handle.net/11676/2OEqomsjwEiAuVuh_pmqXai6 , 2022 Ramonet, M., Delmotte, M., and Lopez, M.: ICOS ATC NRT CH4 growing time series, Saclay (60.0m), 2022-03-01–2022-10-16, https://hdl.handle.net/11676/OFcnDyU5n8teVee7cQE4HQMR , 2022 Ramonet, M., Delmotte, M., and Lopez, M.: ICOS ATC NRT CH4 growing time series, Saclay (100.0m), 2022-03-01–2022-10-16, https://hdl.handle.net/11676/bYoPT0y8E9jQTPz8-3wdKATq , 2022
SMR	Mammarella, I.: ICOS ATC NRT CH4 growing time series, Hyttiälä (16.8m), 2022-03-01–2022-10-16, https://hdl.handle.net/11676/_VIaDFlasf9eqC00lc0Wt8ld , 2022 Mammarella, I.: ICOS ATC NRT CH4 growing time series, Hyttiälä (67.2m), 2022-03-01–2022-10-16, https://hdl.handle.net/11676/OHBTBXX_moBvOamYhLuK91kN , 2022 Mammarella, I.: ICOS ATC NRT CH4 growing time series, Hyttiälä (125.0m), 2022-03-01–2022-10-16, https://hdl.handle.net/11676/8Z0_no6uqvW-Z5-YaxG-p2zu , 2022

SNO	Sørensen, L. L.: ICOS ATC NRT CH4 growing time series, Station Nord (20.0m), 2022-03-01–2022-10-15, https://hdl.handle.net/11676/0VId_7TCnbnB0ewwRq3KKDxA , 2022
	Sørensen, L. L.: ICOS ATC NRT CH4 growing time series, Station Nord (50.0m), 2022-03-01–2022-10-15, https://hdl.handle.net/11676/om8NsBr5VVrBDXEGK6r3Dqk_ , 2022
	Sørensen, L. L.: ICOS ATC NRT CH4 growing time series, Station Nord (85.0m), 2022-03-01–2022-10-15, https://hdl.handle.net/11676/rvVRDSVnmZc8OYVqYW5Ud7WA , 2022
SSL	Schmidt, M., Hoheisel, A., and Meinhardt, F.: ICOS ATC NRT CH4 growing time series, Schauinsland (12.0m), 2022-03-01–2022-10-16, https://hdl.handle.net/11676/WRq3GAacDZ5efGRvXy5INLEh , 2022
	Schmidt, M., Hoheisel, A., and Meinhardt, F.: ICOS ATC NRT CH4 growing time series, Schauinsland (35.0m), 2022-03-01–2022-10-16, https://hdl.handle.net/11676/T0VPT5fzrNglUJHBid_3-XGr , 2022
STE	Kubistin, D., Plaß-Dülmer, C., Kneuer, T., Lindauer, M., and Müller-Williams, J.: ICOS ATC NRT CH4 growing time series, Steinkimmen (32.0m), 2022-03-01–2022-10-16, https://hdl.handle.net/11676/m6ruG6tLLMDKHDxYhBf7fZTC , 2022
	Kubistin, D., Plaß-Dülmer, C., Kneuer, T., Lindauer, M., and Müller-Williams, J.: ICOS ATC NRT CH4 growing time series, Steinkimmen (82.0m), 2022-03-01–2022-10-16, https://hdl.handle.net/11676/FoGwNwIRz6miY_iQAjP2Ii17 , 2022
	Kubistin, D., Plaß-Dülmer, C., Kneuer, T., Lindauer, M., and Müller-Williams, J.: ICOS ATC NRT CH4 growing time series, Steinkimmen (127.0m), 2022-03-01–2022-10-16, https://hdl.handle.net/11676/REnpItg_iiGxHJ5xtWnP_8bw , 2022
	Kubistin, D., Plaß-Dülmer, C., Kneuer, T., Lindauer, M., and Müller-Williams, J.: ICOS ATC NRT CH4 growing time series, Steinkimmen (187.0m), 2022-03-01–2022-10-16, https://hdl.handle.net/11676/UpPwac-1xsF8iv5W5HLCzqXE , 2022
	Kubistin, D., Plaß-Dülmer, C., Kneuer, T., Lindauer, M., and Müller-Williams, J.: ICOS ATC NRT CH4 growing time series, Steinkimmen (252.0m), 2022-03-01–2022-10-16, https://hdl.handle.net/11676/u8RiEqWrtgCYI2-gz3PPHggC , 2022
SVB	Smith, P. and Marklund, P.: ICOS ATC NRT CH4 growing time series, Svartholma (35.0m), 2022-03-01–2022-10-16, https://hdl.handle.net/11676/oMP0-ilovLa_FgN-mn_VE8_a , 2022
	Smith, P. and Marklund, P.: ICOS ATC NRT CH4 growing time series, Svartholma (85.0m), 2022-03-01–2022-10-16, https://hdl.handle.net/11676/wDec3ThQnChg1AJn00AoaUeY , 2022
	Smith, P. and Marklund, P.: ICOS ATC NRT CH4 growing time series, Svartholma (150.0m), 2022-03-01–2022-10-16, https://hdl.handle.net/11676/2Y3LTpc1OkrZeghUt5EDj6g- , 2022
TOH	Kubistin, D., Plaß-Dülmer, C., Kneuer, T., Lindauer, M., and Müller-Williams, J.: ICOS ATC NRT CH4 growing time series, Torfhaus (10.0m), 2022-03-01–2022-10-16, https://hdl.handle.net/11676/CSuR9J0R-G44NUHHOyiSC3bD , 2022
	Kubistin, D., Plaß-Dülmer, C., Kneuer, T., Lindauer, M., and Müller-Williams, J.: ICOS ATC NRT CH4 growing time series, Torfhaus (76.0m), 2022-03-01–2022-10-16, https://hdl.handle.net/11676/ZAQZlwraiwdboq9yq9FgQLUj , 2022
	Kubistin, D., Plaß-Dülmer, C., Kneuer, T., Lindauer, M., and Müller-Williams, J.: ICOS ATC NRT CH4 growing time series, Torfhaus (110.0m), 2022-03-01–2022-10-16, https://hdl.handle.net/11676/p2KhPvHpj7cwkB-MBTTQIIAs , 2022
	Kubistin, D., Plaß-Dülmer, C., Kneuer, T., Lindauer, M., and Müller-Williams, J.: ICOS ATC NRT CH4 growing time series, Torfhaus (147.0m), 2022-03-01–2022-10-16, https://hdl.handle.net/11676/G7UZq17cJOv73PD8C1F6pXa5 , 2022

- TRN Ramonet, M., Lopez, M., and Delmotte, M.: ICOS ATC NRT CH4 growing time series, Trainou (5.0m), 2022-03-01–2022-10-16, <https://hdl.handle.net/11676/OibG252tDcaEI2MOD78vbqgF>, 2022
- Ramonet, M., Lopez, M., and Delmotte, M.: ICOS ATC NRT CH4 growing time series, Trainou (50.0m), 2022-03-01–2022-10-16, <https://hdl.handle.net/11676/05LuKIIgSSNQfFa5L0ZgBVLA>, 2022
- Ramonet, M., Lopez, M., and Delmotte, M.: ICOS ATC NRT CH4 growing time series, Trainou (100.0m), 2022-03-01–2022-10-16, <https://hdl.handle.net/11676/7wYtAL9Y38kh3ED0atWrHhiV>, 2022
- Ramonet, M., Lopez, M., and Delmotte, M.: ICOS ATC NRT CH4 growing time series, Trainou (180.0m), 2022-03-01–2022-10-16, <https://hdl.handle.net/11676/f-MK6g3DvGYhi8kS4-UVQ-Dx>, 2022
- UTO Hatakka, J. and Laurila, T.: ICOS ATC NRT CH4 growing time series, Utö - Baltic sea (57.0m), 2022-03-01–2022-10-16, https://hdl.handle.net/11676/yFO_L2onDwckHg_2194ej4Mx, 2022
- WAO Forster, G. and Manning, A.: ICOS ATC NRT CH4 growing time series, Weybourne (10.0m), 2022-03-01–2022-10-16, <https://hdl.handle.net/11676/YBfukffFk8tReEQDf5sj5sLM>, 2022
- WES Couret, C. and Schmidt, M.: ICOS ATC NRT CH4 growing time series, Westerland (14.0m), 2022-03-01–2022-10-16, <https://hdl.handle.net/11676/5L0cqOHBSQZUPwtzBf-SNXzs>, 2022
- ZEP Lund Myhre, C., Platt, S. M., Hermansen, O., and Lunder, C.: ICOS ATC NRT CH4 growing time series, Zeppelin (15.0m), 2022-03-01–2022-10-16, <https://hdl.handle.net/11676/jRuxDepDwdYIgT6bnMyS1Kb4>, 2022
- ZSF Couret, C. and Schmidt, M.: ICOS ATC NRT CH4 growing time series, Zugspitze (3.0m), 2022-03-01–2022-10-16, <https://hdl.handle.net/11676/Nt6A1n9YgfvESDwZ2tbTu5hE>, 2022